● REVIEW

Advanced diffusion magnetic resonance imaging in patients with Alzheimer's and Parkinson's diseases

Koji Kamagata[1, *], Christina Andica[1], Taku Hatano[2], Takashi Ogawa[2], Haruka Takeshige-Amano[2], Kotaro Ogaki[2], Toshiaki Akashi[1], Akifumi Hagiwara[1], Shohei Fujita[1], Shigeki Aoki[1]

1 Department of Radiology, Juntendo University Graduate School of Medicine, Tokyo, Japan
2 Department of Neurology, Juntendo University School of Medicine, Tokyo, Japan

Abstract

The prevalence of neurodegenerative diseases is increasing as human longevity increases. The objective biomarkers that enable the staging and early diagnosis of neurodegenerative diseases are eagerly anticipated. It has recently become possible to determine pathological changes in the brain without autopsy with the advancement of diffusion magnetic resonance imaging techniques. Diffusion magnetic resonance imaging is a robust tool used to evaluate brain microstructural complexity and integrity, axonal order, density, and myelination via the micron-scale displacement of water molecules diffusing in tissues. Diffusion tensor imaging, a type of diffusion magnetic resonance imaging technique is widely utilized in clinical and research settings; however, it has several limitations. To overcome these limitations, cutting-edge diffusion magnetic resonance imaging techniques, such as diffusional kurtosis imaging, neurite orientation dispersion and density imaging, and free water imaging, have been recently proposed and applied to evaluate the pathology of neurodegenerative diseases. This review focused on the main applications, findings, and future directions of advanced diffusion magnetic resonance imaging techniques in patients with Alzheimer's and Parkinson's diseases, the first and second most common neurodegenerative diseases, respectively.

Key Words: Alzheimer's disease; biomarkers; diffusional kurtosis imaging; disease progression; early diagnosis; free-water imaging; neurites; neurite orientation dispersion and density imaging; Parkinson's disease

Introduction

The prevalence of neurodegenerative diseases with aging as the main risk factor is increasing with an increase in human longevity (Hou et al., 2019). This increasing prevalence of neurodegenerative diseases has resulted in serious medical and socioeconomic problems. The hallmark events in neurodegenerative diseases include misfolding and aggregation of abnormal proteins, which result in cellular stress, synaptic dysfunction, and ultimately neurodegeneration (Soto and Pritzkow, 2018). Although the definitive diagnosis of neurodegenerative diseases is pathologically confirmed via autopsy, living patients are diagnosed according to clinically established diagnostic criteria. However, the frequency of misdiagnosis of these diseases, which are diagnosed only based on clinical symptoms in clinical trials (Salloway et al., 2014), increases the need for objective biomarkers. Recent advances in magnetic resonance imaging (MRI) techniques have made it possible to determine brain pathological changes *in vivo*. In particular, diffusion MRI is a powerful tool used to determine brain microstructural features, such as microstructural complexity, integrity, and axonal order, density, and myelination via the micron-scale displacement of water molecules diffusing in tissues (Beaulieu, 2002). Diffusion tensor imaging (DTI) is a widely utilized diffusion MRI technique in clinical and research settings of neurodegenerative diseases; however, it has several limitations. To overcome these limitations, advanced diffusion MRI techniques, such as diffusional kurtosis imaging (DKI) (Jensen et al., 2005), neurite orientation dispersion and density imaging (NODDI) (Zhang et al., 2012), and free water imaging (FWI) (Pasternak et al., 2009), have recently been proposed. This review focused on the main applications, findings, perspectives, and future directions of advanced diffusion MRI techniques in patients with Alzheimer's disease (AD) and Parkinson's disease (PD), the first and second most common neurodegenerative diseases, respectively.

Search Strategy and Selection Criteria

The MEDLINE database was electronically searched for literature describing advanced diffusion MRI prior to published March 2019 using the following criteria: "neurodegenerative diseases" [All Fields] OR "neurodegenerative disorders" [All Fields] OR "Alzheimer disease" [MeSH Terms] OR "Alzheimer's disease" [All Fields] OR "Parkinson disease" [MeSH Terms] OR "Parkinson's disease" [All Fields] AND ("diffusional kurtosis imaging" [All Fields] OR "neurite orientation dispersion and density imaging"[All Fields] OR "free water" [All Fields] OR "DKI" [All Fields] OR "NODDI" [All Fields] OR "advanced diffusion magnetic resonance imaging" [All Fields]). The studies identified were further screened using the following inclusion criteria: focus on diffusion MRI and the evaluation of AD and/or PD patients. We excluded re-

view articles and studies that did not involve humans or the use of MRI.

One hundred and five studies were identified via MEDLINE search. Based on the inclusion and exclusion criteria, 48 studies were finally selected for this review (**Figure 1**). The selected studies were published between 2013 and 2019, and 60% of them were published within the last three years.

Diffusion MRI Techniques

Diffusion tensor imaging

DTI is a powerful technique used to explore microstructural changes. The theoretical background of DTI has been extensively reviewed (Mori and Zhang, 2006; Assaf and Pasternak, 2008). Briefly, DTI measures the diffusion of water molecules in tissue and provides information about their orientation and quantitative anisotropy (Soares et al., 2013). The diffusion is modeled by a tensor, a mathematical form of a 3×3 symmetric matrix. DTI produces measures, such as fractional aonisotropy (FA; the directionality of water dif-

Figure 1 Flow chart of the article selection process.

fusion), mean diffusivity (MD; the magnitude of diffusion), axial diffusivity (the diffusion rate along the main axis), and radial diffusivity (RD; the transverse diffusion rate) (**Table 1**) (Soares et al., 2013).

The clinical use of DTI, however, is constrained by several limitations: (1) DTI assumes a Gaussian distribution of water molecules (Basser et al., 1994), whereas it is known that biological restrictions in the living tissue microstructure cause deviations from the Gaussian distribution of water molecules (Jensen et al., 2005; Jensen and Helpern, 2010). (2) DTI parameters cannot be used to illustrate specific pathological changes (Assaf and Pasternak, 2008). For example, decreased FA and increased MD may be attributed to demyelination or axonal loss (Chung et al., 2016; Kamagata et al., 2017). Although some studies have demonstrated the usefulness of AD and RD as biomarkers of axonal loss and demyelination, respectively (Beaulieu, 2002), these interpretations have also been questioned in the literature (Wheeler-Kingshott and Cercignani, 2009). (3) The DTI model assumes a single-tissue compartment in each voxel, and thus, the partial volume effect from an extracellular fluid, such as cerebrospinal fluid (CSF) (Alexander et al., 2007), might bias the interpretation of DTI indices (Metzler-Baddeley et al., 2012). (4) DTI is not preferred for the evaluation of gray matter (GM) because of its inability to explore the water diffusion isotropy of GM (Jensen et al., 2005; Jensen and Helpern, 2010).

Diffusional kurtosis imaging

Diffusional kurtosis imaging (DKI) was proposed to overcome the limitations of DTI by estimating the kurtosis of water diffusion based on a probability distribution function. Kurtosis is a dimensionless measure that determines the deviation of the Gaussian distribution of water molecules in a voxel (Jensen et al., 2005). DKI protocols differ from DTI protocols and require at least three b-values (compared with two b-values for DTI), as well as at least 15 diffusion gradient
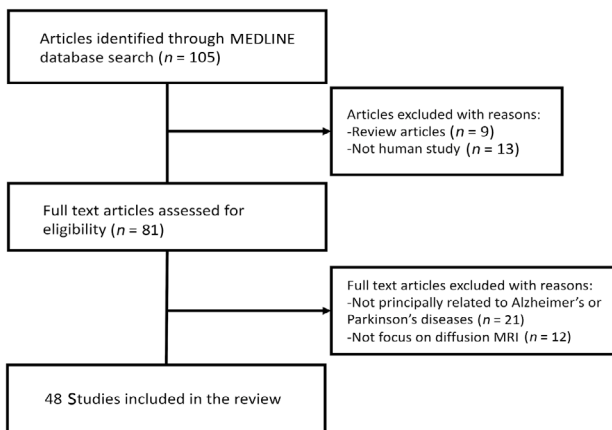
Table 1 Summary of method characteristics

Model	Method	Estimated metrics	Advantages	Disadvantages
Mathematical models	DTI	FA, MD, AxD, RD	Short acquisition time; relatively high reproducibility; easy data acquisition	The estimation of voxels containing multidirectional nerve fibers or free water may not be accurate. Does not reflect specific pathological changes (e.g., demyelination, axonal degeneration)
	DKI	MK, AK, RK	It is not restricted to evaluate the voxels of single fiber populations. Voxels containing multidirectional nerve fibers or gray matter can also be evaluated	Relatively long acquisition time; difficulty in the interpretation of the changes in DKI measures
Biophysical models	NODDI	ICVF, OD, ISOVF	A biological interpretation such as neurite density, neurite orientation dispersion can be provided (needs to be verified)	Long acquisition times to acquire 2 b-shells; relatively low reproducibility: because of the pre-fixed intracellular and extracellular diffusivity, deviations from the fixed value can bias the NODDI measures.
Hybrid models	FWI	FA_T, MD_T, AD_T, RD_T, FW	Can eliminate the effect of partial volume of free water contained in voxels	The voxels containing multidirectional nerve fibers might be considered as FW

AD_T: Free water-corrected AxD; AK: axial kurtosis; AxD: axial diffusivity; DKI: diffusional kurtosis imaging; DTI: diffusion tensor imaging; FA: fractional anisotropy; FA_T: free water-corrected FA; FW: free water; FWI: free-water imaging; ICVF: intracellular volume fraction; ISOVF: isotropic volume fraction; MD: mean diffusivity; MD_T: free water-corrected MD; MK: mean kurtosis; OD: orientation dispersion index; RD: radial diffusivity; RD_T: free water-corrected RD; RK: radial kurtosis.

directions (compared with six b-values for DTI) (Jelescu and Budde, 2017). The test-retest reproducibility of DKI metrics has been demonstrated to be comparable to that of DTI metrics (Shahim et al., 2017). DKI provides the following diffusional kurtosis measures: axial kurtosis (AK), mean kurtosis (MK), and radial kurtosis (RK). Briefly, MK represents the overall microstructural complexity of the brain tissue, whereas AK and RK reflect the tissue complexity along and perpendicular to the direction of water diffusion, respectively (**Table 1**) (Kamagata et al., 2017). Higher kurtosis values indicate greater restriction in tissue, whereas a decrease in kurtosis value might reflect neuronal loss (Arab et al., 2018). In contrast with FA, which can detect the restriction of water diffusion only in anisotropic environments, kurtosis parameters are used to evaluate the restriction of water diffusion both in isotropic and anisotropic environments (Steven et al., 2014). Therefore, DKI is useful in evaluating microstructural changes in the GM (Zhuo et al., 2012) as well as white matter (WM) (Guglielmetti et al., 2016). A major drawback of DKI is that its parameters lack specificity. In line with DTI parameters, it is difficult to interpret the changes in the measures (Kamagata et al., 2016a). Another limitation is that with a shorter imaging protocol, its parameters can vary across brain areas (Szczepankiewicz et al., 2013).

Neurite orientation dispersion and density imaging

NODDI is a multishell diffusion MRI imaging technique that uses a clinically feasible protocol probing the neurite microstructure. The NODDI model assumes three brain tissue compartments, namely intra-neurite (modeled as restricted diffusion), extra-neurite (modeled as hindered diffusion), and free water (modeled as isotropic Gaussian diffusion) compartments (Zhang et al., 2012). Similar to DKI, NODDI also requires at least two shells. NODDI was originally proposed as a two-shell acquisition sequence with 30 gradient directions (711 s/mm² shell) and 60 directions (2855 s/mm² shell) (Zhang et al., 2012). Nevertheless, the single-shell results of orientation dispersion index (ODI) are comparable to the two-shell results (Zhang et al., 2012; Parvathaneni et al., 2018).

Briefly, three NODDI parameters are produced to quantify neurite density [intracellular volume fraction (Vic)], intracellular neurite dispersion (ODI), and the fractional volume of extracellular fluid (isotropic volume fraction) (**Table 1**) (Zhang et al., 2012; Kamagata et al., 2016a). Notably, Vic and ODI are considered two disentangled facets of FA; thus, NODDI provides more specific information of brain microstructure. Furthermore, NODDI parameters can be used to explore the changes in whole brain microstructures, including WM and GM (Zhang et al., 2015).

NODDI measures, particularly ODI, have been found to be less reproducible than DTI measures, and magnetic field strength (i.e., 1.5 and 3 T) has a significant impact on NODDI. Therefore, the data need to be interpreted with caution (Chung et al., 2016). It is important to reiterate that the NODDI model predetermines diffusivity estimation. The model also assumes equal intra- and extracellular diffusivity

(= 1.7 μm²/ms) (Jelescu and Budde, 2017). Because of this oversimplification, any deviation from the fixed values may bias the measures.

Free-water diffusion magnetic resonance imaging

Free-water diffusion MRI (FW diffusion MRI) is a bi-tensor model that allows to differentiate between the water diffusion changes in brain tissue (anisotropic) and those in extracellular space (isotropic) (Pasternak et al., 2009). A single-shell diffusion MRI acquisition can be used to produce FW diffusion MRI measure, and this method can be easily integrated with the pipeline of DTI analysis (Pasternak et al., 2009). The model allows the measurement of FW-corrected DTI parameters, such as FW-corrected FA (FA$_T$), MD (MD$_T$), AD (AD$_T$), and RD (RD$_T$), enabling better specificity for the evaluation of brain tissue (**Table 1**) (Metzler-Baddeley et al., 2012). FW elimination has also been demonstrated to improve DTI-based tractography (Pasternak et al., 2009) and to increase the reproducibility of DTI metrics (Albi et al., 2017).

Importantly, the model allows calculating the fractional volume of extracellular FW within a voxel. Extracellular FW in the human brain exists as CSF and may also accumulate in the extracellular space in brain parenchyma due to brain pathologies (Pasternak et al., 2009; Oestreich et al., 2017). Therefore, the FW map can be potentially used as a biomarker of neuroinflammation (Wang et al., 2011; Andica et al., 2019). Although it is difficult to prove it histopathologically, as neuroinflammation is an active physiological phenomenon, a recent study has demonstrated a relationship between FW in the hippocampus and 18 kDa translocator protein binding, one of the *in vivo* measurements of neuroinflammation (Reid et al., 2019).

Similar to other diffusion techniques, FW diffusion MRI also has some limitations. The bi-tensor model assumes two compartments comprising FW and a single neuronfiber. Since more than 60 percent of brain WM voxels consist of at least two fiber bundles, the signal from fiber bundles that do not match the single fiber tensor will be known as FW, resulting in reduced measure specificity.

Diffusion Applications in Alzheimer's and Parkinson's diseases

Alzheimer's disease

AD is the most common progressive neurodegenerative disease that causes dementia in the elderly individuals. Intracellular neurofibrillary tangles and senile plaques (comprising hyperphosphorylated tau protein and extracellular deposits of β-amyloid peptide, respectively) are considered as the pathological hallmarks of AD. Furthermore, these pathologies could lead to a typical spatiotemporal pattern of synaptic dysfunction and neuronal loss throughout the brain (Aisen et al., 2017). The stages of AD can be broadly divided into three phases. The first is the preclinical phase with no observable clinical symptoms. Subjects with a heritable risk for AD, namely the ε4 allele of apolipoprotein E (APOE ε4)

gene, positive $A\beta_{42}$/CSF tau biomarkers or a parental history of AD, are also considered to have preclinical AD (Hoy et al., 2017). The second phase is the prodromal phase, which is frequently described as mild cognitive impairment (MCI) and carries a higher risk of AD development with a progression rate of 16.5% in 12 months (Petersen, 2004; Petersen et al., 2010). The last phase is the symptomatic phase. It is sometimes difficult to strictly differentiate these phases; therefore, these phases have recently been conceptualized as a multifaceted process moving along a seamless continuum (i.e., AD continuum) (Aisen et al., 2017).

Medial temporal lobe atrophy, as assessed using structural MRI, is currently the gold standard for the early diagnosis of AD (Wang et al., 2015b); nonetheless, the diagnostic accuracy for AD is just moderately high (Schmand et al., 2010). In contrast, advanced diffusion MRI has added further insights into the cerebral microstructural changes related to preclinical, prodromal, and symptomatic AD (Parente et al., 2008).

Applications of advanced diffusion magnetic resonance imaging in Alzheimer's disease

DKI has consistently been reported to be useful for detecting microstructural changes in cerebral WM in patients with MCI and AD (Falangola et al., 2013; Gong et al., 2013; Benitez et al., 2014; Struyfs et al., 2015; Yuan et al., 2016; Chen et al., 2017). Furthermore, some previous studies have reported that this technique is useful for detecting GM alterations (Yuan et al., 2016; Gong et al., 2017; Wang et al., 2018; Song et al., 2019). Reductions in DKI parameters in the corpus callosum (Struyfs et al., 2015), corona radiata (Falangola et al., 2013; Struyfs et al., 2015), cingulate bundle (Yuan et al., 2016), hippocampus (Yuan et al., 2016; Gong et al., 2017; Song et al., 2019), and deep GM (Yuan et al., 2016; Gong et al., 2017; Wang et al., 2018) in patients with AD and MCI relative to the findings in healthy controls have been reported.

Gong et al. (2013) first utilized DKI to evaluate microstructural changes in cerebral WM and GM in patients with MCI and AD. They found significantly decreased MK and RK in parietal WM and decreased AK in occipital GM in patients with AD compared with patients with MCI.

In addition, significant correlations were found between DKI measures and the mini-mental scale examination score in both GM and WM in these areas. Furthermore, Gong et al. (2017) focused on capturing microstructural anomalies in GM in patients with AD using DKI and compared DKI metrics against cortical thickness and deep GM volume. They found decreased MK in patients with MCI relative to the findings in healthy controls in the globus pallidus, putamen, thalamus, and hippocampus. On the other hand, significant atrophy was observed only in the bilateral amygdala and hippocampi at the MCI relative to the control data (**Figure 2**). The findings were considered due to loss of microstructural compartments in patients with MCI, such as neuronal somas, dendrite axons, and synapses in GM. In a previous study focusing on the hippocampus (Wang et al., 2015a), significantly lower MK values were found in patients with MCI and AD than in healthy subjects with no difference in hippocampal volume between the MCI and healthy subjects (Wang et al., 2015a). These findings suggest that microstructural changes detected by DKI may precede brain atrophies. On the other hand, Falangola et al. (2013) also utilized DKI to detect brain microstructural changes in patients with MCI or AD and in healthy controls. Among patients with MCI and AD, they found a decrease in all DKI parameters in the anterior corona radiata compared with the findings in cognitively intact healthy controls. Furthermore, the mean and radial diffusion kurtosis values in the anterior corona radiata were shown as the best parameters for differentiating MCI from controls in ROC analyses. This result suggests that DKI may be useful for assessing microstructural changes in the early stage of MCI.

Only three studies have used NODDI to evaluate the brain microstructure of patients with AD (Slattery et al., 2017; Parker et al., 2018; Fu et al., 2019). Two studies evaluated early-onset AD using NODDI (Slattery et al., 2017; Parker et al., 2018), whereas one study evaluated MCI/AD (Fu et al., 2019). These studies have reported the utility of NODDI to evaluate AD pathology. Slattery et al. (2007) investigated WM alteration related to apolipoprotein (APOE) ε4 modulation in 37 patients with young-onset AD (59% were positive for APOE ε4) and 23 healthy subjects to understand the mechanisms underlying heterogeneity in phenotype of young-onset AD. They found that WM alteration, as detected by DTI or NODDI, was more extensive in patients with ε4$^+$ early-onset AD but more focal in those with ε4$^-$ early-ly-onset AD (**Figure 3**). The authors further observed that the decreased FA in WM in patients with early-onset AD was attributable to the effects of either a decrease in Vic (i.e., a decrease in neurite density) or an increase in OD (i.e., a degree in neurite orientation dispersion). The microstructural alteration of cortical GM in patients with early-onset AD was also evaluated using NODDI (Parker et al., 2018). In this study, Vic, OD, and cortical thickness in the cortical areas related to early atrophy in AD (i.e., entorhinal area, inferior temporal cortex, middle temporal cortex, fusiform cortex, and precuneus) and one area relatively spared from atrophy in AD (precentral cortex) were compared between controls and patients. Vic was significantly decreased in patients with early-onset AD in all regions, whereas cortical thickness was significantly decreased in the AD group in regions associated with early atrophy in AD but not in the precentral cortex (**Figure 4**). Furthermore, cortical Vic was significantly associated with mini-mental scale examination scores in the patient group. These results indicate that cortical Vic and ODI might be more sensitive markers for cortical assessment than cortical thickness.

FWI has been applied to evaluate the cerebral pathology of the preclinical stages of AD and MCI and the symptomatic phase of AD, and its usefulness has been reported (Hoy et al., 2017; Ji et al., 2017, 2019; Montal et al., 2018). Hoy et al. (2017) investigated the association between FWI parameters and AD-related CSF biomarkers (pTau$_{181}$, $A\beta_{42}$, YKL-40, sAPPβ, and tTau) in 70 subjects with preclinical AD (APOE ε4 and parental history of AD) and found that FW content
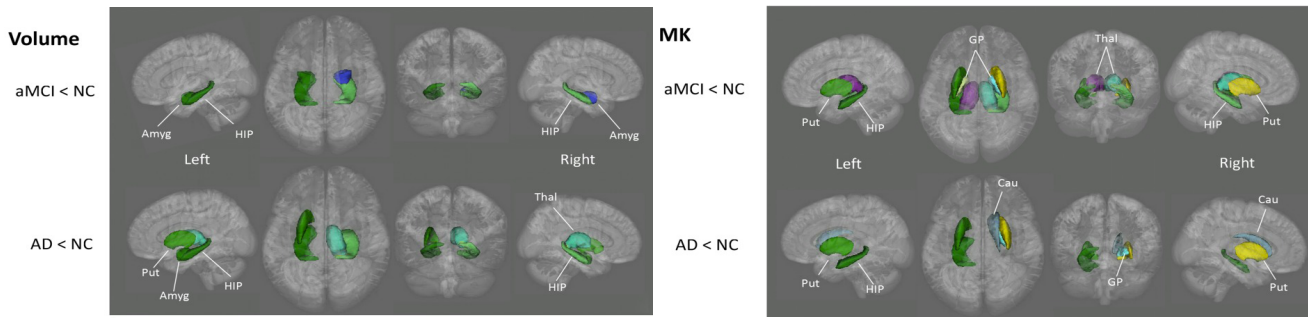
Figure 2 Lower volume and mean kurtosis (MK) are demonstrated in the deep gray matter areas of patients with amnestic mild cognitive impairment (aMCI) and Alzheimer's disease (AD) when compared with controls.
Reproduced with permission from Gong et al., 2017. Amyg: Amygdala; Cau: caudate nucleus; GP: Globus pallidus; HIP: hippocampus; NC: normal control; Put: putamen; Thal: thalamus.
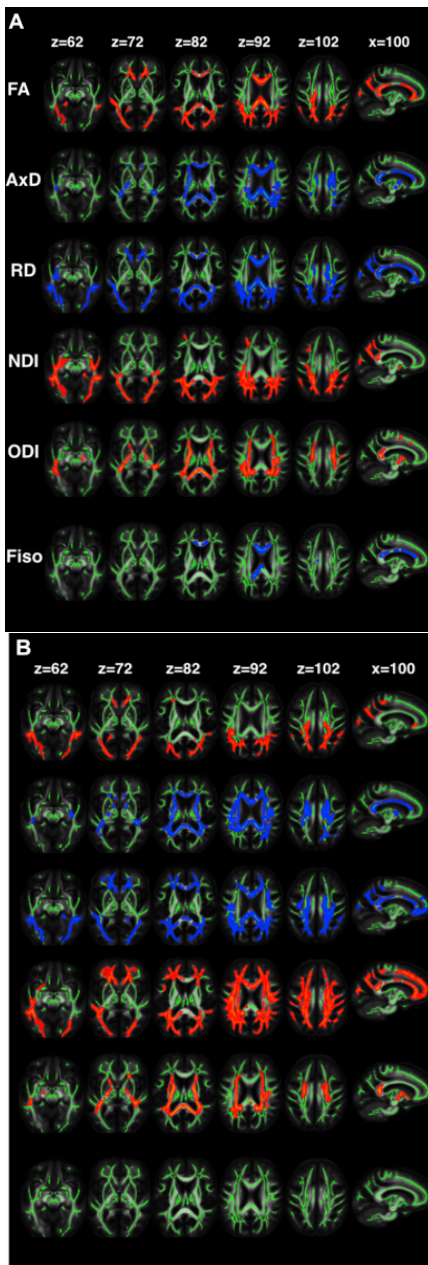

Figure 3 The changes in diffusion tensor imaging (FA, axial diffusivity, and RD), neurite orientation dispersion, and density imaging (NDI, ODI, and Fiso) metrics in patients with (A) ε4⁻ and (B) ε4⁺ young-onset Alzheimer's disease in comparison with controls.
In the voxel-wise group differences, the metrics that are increased and decreased in patients are highlighted in blue and red, respectively. The results are overlaid on axial and sagittal planes of the white matter skeleton (shown in green) in the neurologic convention. Reproduced with permission from Slattery et al., 2017 (CC BY 4.0). AxD: Axial diffusivity; FA: fractional anisotropy; Fiso: fraction of isotropic water; L: left; NDI: neurite density index; ODI: orientation dispersion index; R: right; RD: radial diffusivity.
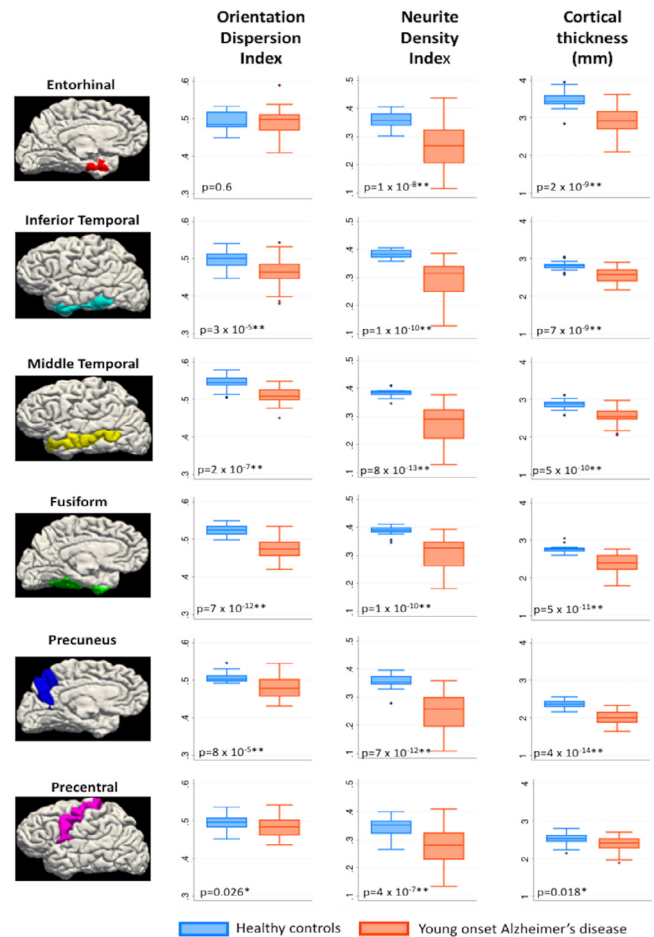
Figure 4 Box plots of orientation dispersion index, neurite density index, and cortical thickness in patients with young-onset Alzheimer's disease and healthy controls in six cortical regions of interests.
$*P < 0.05$, $**P < 0.008$. Bonferroni-corrected: $P = 0.008$ (0.05/6). Reproduced with permission from Parker et al., 2018 (CC BY 4.0).

derived from FWI was correlated with these CSF biomarkers in WM regions, including the frontal, temporal, and parietal lobes. These findings suggest that FWI can provide increased sensitivity to early cerebral WM changes associated with AD pathology. Furthermore, because YKL-40 is known as a CSF marker of microglial activation and neuroinflammation (Hoy et al., 2017), FW parameters might be used as markers of neuroinflammation. In contrast, FW changes in cortical GM have also been proposed as a biomarker for AD (Montal et al., 2018). The authors evaluated cortical microstructural changes along the AD continuum using FWI. They assessed changes in cortical MD, FW, and thickness in healthy control subjects (*n* = 254), patients with MCI (*n* = 41), and patients with AD (*n* = 31). They classified healthy controls into stages 0, 1, and 2/3 following the National Institute on Aging-Alzheimer's Association stages. They demonstrated the biphasic trajectory of changes in FW and cortical thickness. Subjects in stage 1 displayed increased cortical thickness and decreased FW compared with the findings in stage 0 subjects. Stage 2/3 subjects exhibited decreased cortical thickness and increased cortical FW, whereas the changes were more widespread in patients with AD. They considered that increased cortical thickness and decreased in FW in the early preclinical stage of AD might be related to an amyloid-induced inflammatory response. One explanation is that inflammation causes changes in cell volume resulting in cortical thickening and cell number changes (glia recruitment and activation), which induces decrease in cortical FW.

In addition, disruption of WM structural connectivity, which is related to myelinated axon and synaptic degeneration, in patients with AD has been demonstrated using diffusion MRI and graph theory. Mallio et al. (2015) showed disconnectivity around the entorhinal cortex and hippocampus in patients with MCI and AD and wide pathology in patients with AD. Recently, Kim et al. (2019) evaluated the longitudinal data of patients with preclinical AD and analyzed the correlation between WM neural networks and CSF biomarkers of AD. They observed an association between increased longitudinal changes in WM connectivity and elevated CSF biomarker levels.

However, it is also important to reiterate that in some patients, MCI will progresses to non-AD diseases, such as frontotemporal dementia or Lewy body dementia (Petersen, 2009). Therefore, future longitudinal studies using advanced diffusion MRI techniques should be conducted in patients with MCI that progresses to AD, such as AD Neuroimaging Initiative (ADNI) database (Petersen et al., 2010), to demonstrate the robustness of these methods as early biomarkers of AD.

Parkinson's diseases
PD is the second most common progressive neurodegenerative disorder and is characterized by the selective loss of dopaminergic neurons in the substantia nigra (SN) as well as motor symptoms, such as bradykinesia, rigidity, and tremors. However, recent neuropathological studies indicate that Lewy pathology, the pathological hallmark of PD, initially begins in the enteric nervous system or the olfactory bulb and then spreads to the SN, limbic areas, striatum, insular cortex and neocortex (Braak et al., 2002, 2003, 2004; Braak and Del Tredici, 2008). Furthermore, another study has reported that cardiac denervation precedes nigrostriatal dopaminergic degeneration (Salsone et al., 2012). Because it is becoming clear that the damage of neuronal populations other than the nigral dopaminergic neurons is associated with various non-motor symptoms of PD such as olfactory impairment, sleep disorders, autonomic dysfunction, and cognitive impairment, the classical view that PD is characterized only by the selective damage of dopaminergic neurons in the SN has been replaced by the view that PD is a severe systemic neurodegenerative disorder (Klingelhoefer and Reichmann, 2017).

Considering that pathological changes have already begun in areas other than the brain, such as the enteric and sympathetic nervous systems, it is expected that it will be difficult to use brain MRI for the early diagnosis of PD. However, development of techniques, such as advanced diffusion MRI, has been shown to be useful in differentiating PD from atypical Parkinsonism as well as for the early detection of alterations within the SN and other brain regions. SN changes are considered an important landmark in the progression of PD because progressive dopaminergic neuron loss (up to 70% of dopamine neurons have been lost by the time of the first diagnosis) in this area leads to the motor symptoms of PD (Cheng et al., 2010). The widespread aggregation of α-synuclein in the form of Lewy neurites and Lewy bodies is also considered an important pathological cause of PD (Fearnley and Lees, 1991; Braak et al., 2003). PD involves multiple neurotransmitter pathways that cause numerous non-motor symptoms (Schapira et al., 2017).

The development of reliable early biomarkers may be helpful for the development of neuroprotective treatments, which are essential for slowing the progress of PD. Indeed, advanced diffusion MRI, such as DKI, NODDI, and FWI, has demonstrated the remarkable advantages of DTI in the assessment of the microstructural changes in PD in the SN, WM, and GM, as observed in prior studies.

Applications of advanced diffusion magnetic resonance imaging in Parkinson's disease
Lower MK in the putamen was associated with severe motor and cognitive impairment in patients with PD (Surova et al., 2016). Furthermore, using DKI, Zhang et al. (2019) demonstrated a correlation between hyperhomocysteinemia (HHCY) and the SN structural changes in PD. In their study, they recorded longitudinal changes in SN in patients with PD, including significantly worse HHCY compared with the findings in the PD control group. Zhang et al. (2016) evaluated patients with PD with and without striatal silent lacunar infarction (SSLI) using DKI. MK values of SN in the PD with SSLI group were found to be higher than those in the PD without SSLI group. In addition, the frequency of SSLI had a linear correlation with the MK values of the SN. The findings indicate that SSLI in early-stage PD is associated with SN

microstructural changes, and these changes can be detected via DKI. In another study, MK in the brainstem structures was also identified as an effective biomarker for differentiating PD from other atypical Parkinsonism with sensitivity and specificity of greater than 80% (Ito et al., 2017).

Decreased Vic was found in the contralateral SN pars compacta and putamen of patients with PD compared with the findings in healthy subjects. Vic also showed the best diagnostic performance among DTI and other NODDI measures using receiver operating characteristics curve analysis (**Figure 5**). Significant negative correlations were also found between Vic and OD in the SN pars compacta and disease severity (Kamagata et al., 2016b). Another study demonstrated retrograde degeneration in patients with PD, as shown by decreased Vic in the contralateral distal part of the nigrostriatal pathway (Andica et al., 2018).

Increased FW levels have been consistently demonstrated in single- and multi-site studies in the posterior SN of patients with PD and have been comparable with the findings in healthy controls (Ofori et al., 2015a, 2017; Planetta et al., 2016; Arribarat et al., 2019; Mitchell et al., 2019; Yang et al., 2019). In a prospective longitudinal study, FW levels increased in the posterior SN with the progression of PD over 1 (Ofori et al., 2015b) and 4 years (Burciu et al., 2017), whereas FW values did not change in healthy controls. Meanwhile, in a later-stage PD cohort, increased FW levels over a 3 years of follow-up period were demonstrated in the anterior SN, but not in the posterior SN, potentially reflecting the posterior-to-anterior pattern of SN degeneration over the progression of PD (Guttuso et al., 2018). The longitudinal changes of FW also predicted subsequent changes in bradykinesia (Ofori et al., 2015b) and Hoehn and Yahr staging scale (Burciu et al., 2017).

Patients with PD who had taken rasagiline (monoamine oxidase type B inhibitor) had higher FW levels in the posterior SN than healthy controls but lower levels than those with PD who had not taken rasagiline (Burciu et al., 2016). These findings suggest that extracellular dopamine levels are higher in patients with PD who received rasagiline than those in patients who did not receive the drug (Burciu et al., 2016). Significant differences in FW and FAT were not observed between OFF and ON antiparkinsonian medication, suggesting that both parameters reflect the chronic stage of SN microstructural changes (Chung et al., 2017). In a different study, Yang et al. (2019) reported a negative correlation between FW values in the SN and striatal vesicular monoamine transporter 2, indicating that nigral microstructural changes detected using FWI correlated with the neuronal loss of striatal dopaminergic neurons. Furthermore, they found that higher Hoehn and Yahr stage, MDS-UPDRS part III total scores, and posture and gait scores were correlated with increased FW values in the posterior part of the SN and decreased vesicular monoamine transporter type 2 binding in the putamen. Furthermore, in patients with moderate-stage PD, Arribarat et al. (2019) noted increased relaxometry T2* (reflecting iron deposition) in the anterior SN and elevated FW and MDT values in the posterior SN. They

suggested that the results reflect the complementary aspect of the two parameters and represent different pathophysiological processes in PD.

A study of 44 patients with PD and 24 healthy controls using FWI and NODDI observed increased FW and isotropic volume fraction in the posterior part of the SN (Mitchell et al., 2019). This study also demonstrated high accuracies of NODDI (area under the curve = 0.945) and FWI (area under the curve = 0.969) in differentiating PD from atypical Parkinsonism (such as multiple-system anisotropy Parkinsonian variant and progressive supranuclear palsy), with no significant difference between models (**Figure 6**; Mitchell et al., 2019).

In WM, DKI displayed greater sensitivity than DTI by revealing more extensive microstructural changes in the PD group than in the control group. Decreased MK was found in the frontal, occipital, parietal, and right temporal WM, whereas decreased FA was only observed in the frontal WM. In addition, lower MK was demonstrated in crossing fiber areas such as the superior longitudinal fasciculus and posterior corona radiata (Kamagata et al., 2014). A separate study of the anterior and posterior cingulate fiber (Kamagata et al., 2013) noted decreased MK and FA in the anterior cingulate fiber of patients with PD, whereas MK exhibited the best diagnostic performance. The anterior cingulum is expected to display changes in early-stage PD, suggesting that DKI measures can be used as an early biomarker of PD.

Kamagata et al. (2017) used NODDI and DKI to assess GM in patients with PD, and demonstrated changes in NODDI (reduced Vic and increased VISO) and DKI (reduced MK, AK, and RK) parameters when compared with healthy controls in areas related to Braak stages IV and V. The changes may be related to the sparing of neurite structures and neuronal loss in GM. Furthermore, the changes of NODDI and DKI parameters were more extensive than those of DTI parameter (i.e., reduced FA and increased AD, MD, and RD), indicating that NODDI and DKI have higher sensitivity compared to DTI for detecting GM anomalies in patients with PD (**Figure 7**). In addition, NODDI and DKI measures in some GM areas, such as frontal, temporal, basal ganglia, limbic, and paralimbic areas were correlated with UPDRS-III scores.

In WM and GM in patients with PD, changes in FWI measures were demonstrated in more specific WM areas compared with DTI indices. Specifically, compared with the findings in healthy controls, reduced FAT and increased MDT, ADT, and RDT values were predominantly demonstrated in the anterior WM areas; meanwhile, increased FW levels were recorded in the posterior WM areas of patients with PD. Patients with PD also displayed increased MDT, ADT, and FW levels in GM regions related to Braak stage IV, whereas no significant changes were observed in DTI measures. These findings indicate that in WM in patients with PD, neuroinflammation precedes axonal degeneration. Further, the FW imaging indices seem to be more sensitive than DTI indices in evaluating GM changes in patients with PD (Andica et al., 2019).

Similar to AD, PD is also considered a multifactorial disease related to the disruption of WM connectivity. Diffusion MRI has also been used to evaluate neural networks in patients with PD using graph theory analyses. To date, Nigro et al. (2016) and Kamagata et al. (2018) have demonstrated decreased WM connectivity in motor and non-motor regions in patients with PD compared with healthy controls.

Challenges and Future Directions

As described in this review, advanced diffusion MRI techniques, including DKI, FWI, and NODDI, have provided new insights into the *in vivo* assessment of the brain microstructure in neurodegenerative diseases. However, clinical evidence regarding advanced diffusion MRI is lacking, unlike routine DWI, which is currently used in clinical practice to assess acute infarction. In addition, cost-effectiveness must also be considered. Although using hippocampal volume as a biomarker of AD has been shown to reduce the required sample size and cost of clinical trials in AD (Yu et al., 2014), advanced diffusion MRI lacks similar data.

There are several limitations to overcome to consider advanced diffusion MRI, a biomarker that can be used for clinical trials. First, the sample size of the studies demonstrating the utility of these techniques was small. Therefore, large-scale, multi-site studies are required to establish evidence for the use of DKI, FWI, and NODDI as biomarkers for neurodegenerative diseases. In addition, MRI scanner types, imaging parameters, post-processing algorithms, and magnetic fields are often different for each imaging site (Zhu et al., 2011). These differences might explain the data incompatibility. For example, it has been reported that NODDI parameters differ between 1.5 and 3T MRI (Chung et al., 2016). In fact, the mean percentage change with increasing field strength of Vic was reported as 10.26–15.02%, whereas the mean percentage change of ODI has been reported as −10.62 to −8.34%. Further, Cercignani et al. (2003) evaluated the inter-sequence variability of diffusion MRI data obtained using three different sequences for eight healthy subjects. They observed inter-sequence variability, measured via coefficient of variation, of 5.45–7.34% for FA. Conversely, Kamagata et al. (2015) investigated inter-site reliability using identical 3T MRI scanners and acquisition protocols at two different sites. They reported that the coefficient of variation ranged between 0.6% and 5.6%. These non-linear variations of diffusion MRI parameters across sites reduced statistical power (Zhu et al., 2011). Therefore, standard imaging protocols and post-processing algorithms are required to reduce the inter-site variability of diffusion MRI parameters. For example, a model-free post-processing algorithm can be used for direct harmonization of diffusion MRI and for reducing site-specific variations (Huynh et al., 2019). The authors demonstrated that the method could minimize the variations (from 1% to 3% to less than 0.9%) of DTI parameters (FA and MD) of traveling human subjects scanned at multiple sites. A similar post-processing method might be validated in a multi-center large cohort study. Second, the relationships between the changes in DKI, FWI, and NODDI parameters and pathological changes in patients with neurodegenerative diseases are not fully understood. Because DKI, FWI, and NODDI remain models for estimating the microstructures of brain tissue, postmortem studies of human or animal models of neurodegenerative disease are necessary to address the relationships between these parameters and pathological findings. These limitations should be overcome to permit the use of advanced diffusion MRI as a biomarker for evaluating neurodegenerative diseases.

Open peer reviewer: *George D. Vavougios, University of Thessaly, Greece.*
Additional file: *Open peer review report 1.*

References

Aisen PS, Cummings J, Jack CR Jr, Morris JC, Sperling R, Frölich L, Jones RW, Dowsett SA, Matthews BR, Raskin J, Scheltens P, Dubois B (2017) On the path to 2025: understanding the Alzheimer's disease continuum. Alzheimers Res Ther 9:60.

Albi A, Pasternak O, Minati L, Marizzoni M, Bartrés-Faz D, Bargalló N, Bosch B, Rossini PM, Marra C, Müller B, Fiedler U, Wiltfang J, Roccatagliata L, Picco A, Nobili FM, Blin O, Sein J, Ranjeva JP, Didic M, Bombois S, et al. (2017) Free water elimination improves test-retest reproducibility of diffusion tensor imaging indices in the brain: A longitudinal multisite study of healthy elderly subjects. Hum Brain Mapp 38:12-26.

Alexander AL, Lee JE, Lazar M, Field AS (2007) Diffusion tensor imaging of the brain. Neurotherapeutics 4:316-329.

Andica C, Kamagata K, Hatano T, Okuzumi A, Saito A, Nakazawa M, Ueda R, Motoi Y, Kamiya K, Suzuki M, Hori M, Kumamaru KK, Hattori N, Aoki S (2018) Neurite orientation dispersion and density imaging of the nigrostriatal pathway in Parkinson's disease: Retrograde degeneration observed by tract-profile analysis. Parkinsonism Relat Disord 51:55-60.

Andica C, Kamagata K, Hatano T, Saito A, Uchida W, Ogawa T, Takeshige-Amano H, Zalesky A, Wada A, Suzuki M, Hagiwara A, Irie R, Hori M, Kumamaru KK, Oyama G, Shimo Y, Umemura A, Pantelis C, Hattori N, Aoki S (2019) Free-water imaging in white and gray matter in Parkinson's disease. Cells doi: 10.3390/cells8080839.

Arab A, Wojna-Pelczar A, Khairnar A, Szabo N, Ruda-Kucerova J (2018) Principles of diffusion kurtosis imaging and its role in early diagnosis of neurodegenerative disorders. Brain Res Bull 139:91-98.

Arribarat G, Pasternak O, De Barros A, Galitzky M, Rascol O, Peran P (2019) Substantia nigra locations of iron-content, free-water and mean diffusivity abnormalities in moderate stage Parkinson's disease. Parkinsonism Relat Disord 65:146-152.

Assaf Y, Pasternak O (2008) Diffusion tensor imaging (DTI)-based white matter mapping in brain research: a review. J Mol Neurosci 34:51-61.

Basser PJ, Mattiello J, LeBihan D (1994) Estimation of the effective self-diffusion tensor from the NMR spin echo. J Magn Reson B 103:247-254.

Beaulieu C (2002) The basis of anisotropic water diffusion in the nervous system - a technical review. NMR Biomed 15:435-455.
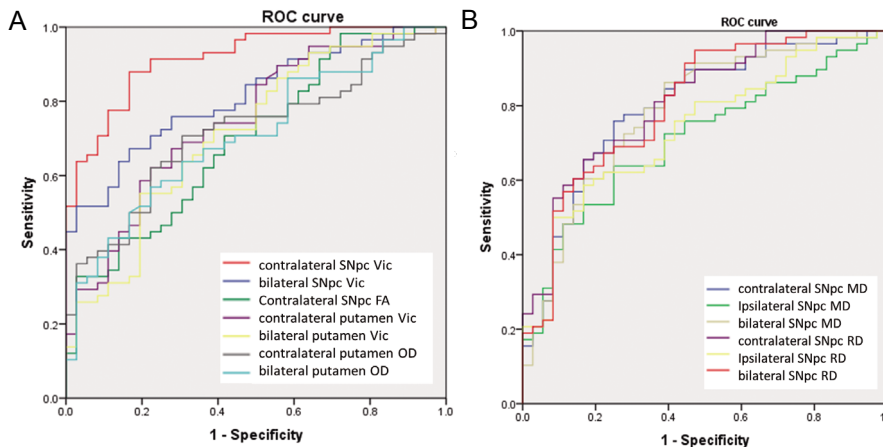
Figure 5 Receiver operating characteristics.
Receiver operating curves of Vic and OD in the SNpc and putamen (A), the Vic at the contralateral SNpc had the greatest sensitivity and specificity, and the MD and RD (B) at the SNpc. FA: Fractional anisotropy; MD: mean diffusivity; OD: orientation dispersion index; RD: radial diffusivity; ROC: receiver operating charactentic fractional qnisotropy; SNpc: substantia nigra pars compacta; Vic: intracellular volume fraction. Reproduced with permission from Kamagata et al., 2016b.

NODDI: SCP (Viso), MCP (Vic), LB V (Viso), GP (ODI), THA (Vic)
FW$_{ms}$: SCP (FW), CN (FW), MCP (FW), STN (FW), CC1 (FW)
FW$_{ss}$: SCP (FW), CN (FW), MCP (FW), CC1 (FW), STN (FW), LB VI (FW), GP (FAt), LB V (FW), DN (FW)
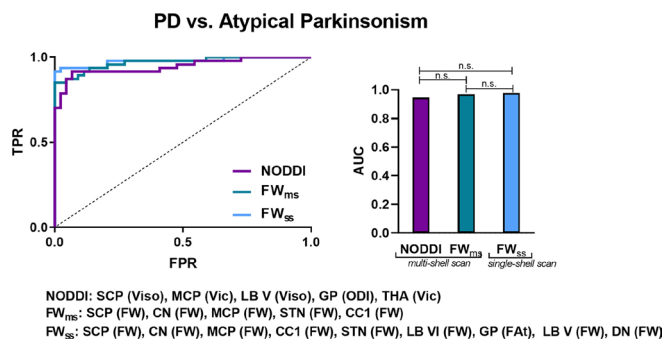
Figure 6 Receiver operating curve analyses and corresponding area under the curve for each diffusion imaging model for differentiating Parkinson's disease (PD) from atypical Parkinsonism (multiple-system anisotropy Parkinsonian variant and progressive supranuclear palsy).
Delong's test was conducted to determine between-model differences. CC1: Corpus callosum prefrontal area; CN: caudate nucleus; DN: dentate nucleus; FWms: free water derived from the multishell scan; FAt$_{ms}$: free water-corrected fractional anisotropy derived from the multi-shell scan; FAtss: free water-corrected fractional anisotropy derived from the single-shell scan; FPR: false positive rate; FWss: free water derived from the single-shell scan; GP: globus pallidus; LBV: cerebellar lobule V; LB VI: cerebellar lobule VI; MCP: middle cerebellar peduncle; n.s.: not significant; ODI: orientation dispersion index; SCP: superior cerebellar peduncle; STN: subthalamic nucleus; THA: thalamus; TPR: true positive rate; Vic: intracellular volume fraction; Viso: isotropic volume fraction. Reproduced with permission from Mitchell et al., 2019.
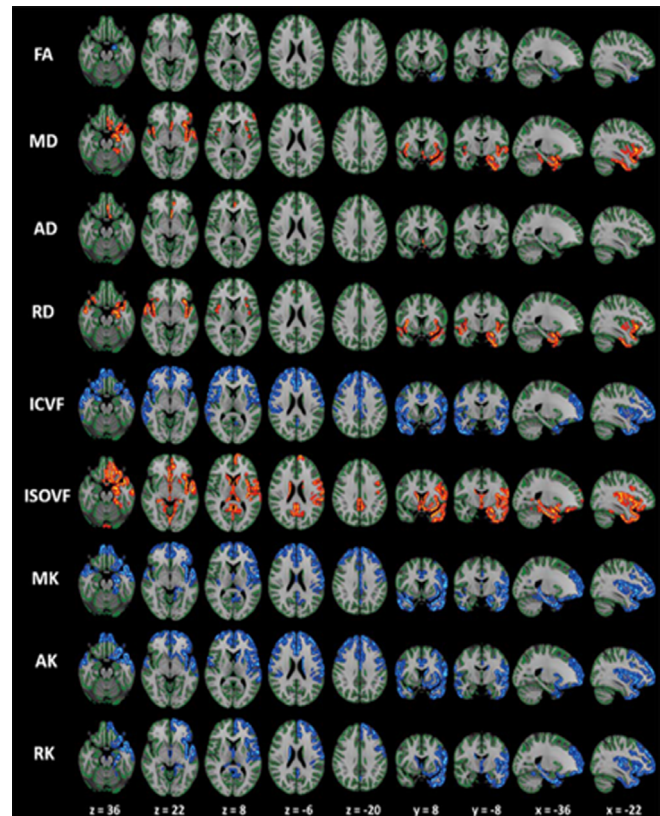

Figure 7 The gray-matter based spatial statistics (GBSS) analysis of diffusion tensor imaging (DTI), diffusional kurtosis imaging, and neurite orientation dispersion, and density imaging metrics in patients with Parkinson's disease (PD) versus controls.
Patients with PD demonstrated reduced FA, ICVF, MK, AK, and RK (highlighted in blue-light blue colors) and increased MD, AD, RD, and ISOVF (highlighted in red-yellow colors) compared with the age-matched healthy subjects. In patients with PD, the changes of ICVF, MK, AK, and RK were measured in the limbic, paralimbic, frontal, and temporal cortical gray matter. The changes in the conventional DTI parameters (FA, AD, and RD) were noticeably smaller than those in MK, AK, RK, and ICVF. The results are enhanced (corrected $P < 0.05$) for visualization using using the fill script implemented in FSL. AD: Axial diffusivity; AK: axial kurtosis; FA: fractional anisotropy; ICVF: intracellular volume fraction; ISOVF: isotropic volume fraction; MD: mean diffusivity; MK: mean kurtosis; OD: orientation dispersion index; RD: radial diffusivity; RK: radial kurtosis. Reproduced with permission from Kamagata et al., 2017.

Benitez A, Fieremans E, Jensen JH, Falangola MF, Tabesh A, Ferris SH, Helpern JA (2014) White matter tract integrity metrics reflect the vulnerability of late-myelinating tracts in Alzheimer's disease. Neuroimage Clin 4:64-71.

Braak H, Del Tredici K (2008) Invited Article: Nervous system pathology in sporadic Parkinson disease. Neurology 70:1916-1925.

Braak H, Del Tredici K, Bratzke H, Hamm-Clement J, Sandmann-Keil D, Rub U (2002) Staging of the intracerebral inclusion body pathology associated with idiopathic Parkinson's disease (preclinical and clinical stages). J Neurol 249:1-5.

Braak H, Del Tredici K, Rub U, de Vos RA, Jansen Steur EN, Braak E (2003) Staging of brain pathology related to sporadic Parkinson's disease. Neurobiol Aging 24:197-211.

Braak H, Ghebremedhin E, Rub U, Bratzke H, Del Tredici K (2004) Stages in the development of Parkinson's disease-related pathology. Cell Tissue Res 318:121-134.

Burciu RG, Ofori E, Archer DB, Wu SS, Pasternak O, McFarland NR, Okun MS, Vaillancourt DE11 (2017) Progression marker of Parkinson's disease: a 4-year multi-site imaging study. Brain 140:2183-2192.

Burciu RG, Ofori E, Shukla P, Pasternak O, Chung JW, McFarland NR, Okun MS, Vaillancourt DE (2016) Free-water and BOLD imaging changes in Parkinson's disease patients chronically treated with a MAO-B inhibitor. Hum Brain Mapp 37:2894-2903.

Cercignani M, Bammer R, Sormani MP, Fazekas F, Filippi M (2003) Inter-sequence and inter-imaging unit variability of diffusion tensor MR imaging histogram-derived metrics of the brain in healthy volunteers. AJNR Am J Neuroradiol 24:638-643.

Chen Y, Sha M, Zhao X, Ma J, Ni H, Gao W, Ming D (2017) Automated detection of pathologic white matter alterations in Alzheimer's disease using combined diffusivity and kurtosis method. Psychiatry Res Neuroimaging 264:35-45.

Cheng HC, Ulane CM, Burke RE (2010) Clinical progression in Parkinson disease and the neurobiology of axons. Ann Neurol 67:715-725.

Chung AW, Seunarine KK, Clark CA (2016) NODDI reproducibility and variability with magnetic field strength: A comparison between 1.5 T and 3 T. Hum Brain Mapp 37:4550-4565.

Chung JW, Burciu RG, Ofori E, Shukla P, Okun MS, Hess CW, Vaillancourt DE (2017) Parkinson's disease diffusion MRI is not affected by acute antiparkinsonian medication. Neuroimage Clin 14:417-421.

Falangola MF, Jensen JH, Tabesh A, Hu C, Deardorff RL, Babb JS, Ferris S, Helpern JA (2013) Non-Gaussian diffusion MRI assessment of brain microstructure in mild cognitive impairment and Alzheimer's disease. Magn Reson Imaging 31:840-846.

Fearnley JM, Lees AJ (1991) Ageing and Parkinson's disease: substantia nigra regional selectivity. Brain 114:2283-2301.

Fu X, Shrestha S, Sun M, Wu Q, Luo Y, Zhang X, Yin J, Ni H (2019) Microstructural white matter alterations in mild cognitive impairment and Alzheimer's disease: study based on Neurite Orientation Dispersion and Density Imaging (NODDI). Clin Neuroradiol doi: 10.1007/s00062-019-00805-0.

Gong NJ, Chan CC, Leung LM, Wong CS, Dibb R, Liu C (2017) Differential microstructural and morphological abnormalities in mild cognitive impairment and Alzheimer's disease: Evidence from cortical and deep gray matter. Hum Brain Mapp 38:2495-2508.

Gong NJ, Wong CS, Chan CC, Leung LM, Chu YC (2013) Correlations between microstructural alterations and severity of cognitive deficiency in Alzheimer's disease and mild cognitive impairment: a diffusional kurtosis imaging study. Magn Reson Imaging 31:688-694.

Guglielmetti C, Veraart J, Roelant E, Mai Z, Daans J, Van Audekerke J, Naeyaert M, Vanhoutte G, Delgado YPR, Praet J, Fieremans E, Ponsaerts P, Sijbers J, Van der Linden A, Verhoye M (2016) Diffusion kurtosis imaging probes cortical alterations and white matter pathology following cuprizone induced demyelination and spontaneous remyelination. Neuroimage 125:363-377.

Guttuso T Jr, Bergsland N, Hagemeier J, Lichter DG, Pasternak O, Zivadinov R (2018) Substantia nigra free water increases longitudinally in Parkinson disease. AJNR Am J Neuroradiol 39:479-484.

Hou Y, Dan X, Babbar M, Wei Y, Hasselbalch SG, Croteau DL, Bohr VA (2019) Ageing as a risk factor for neurodegenerative disease. Nat Rev Neurol 15:565-581.

Hoy AR, Ly M, Carlsson CM, Okonkwo OC, Zetterberg H, Blennow K, Sager MA, Asthana S, Johnson SC, Alexander AL, Bendlin BB (2017) Microstructural white matter alterations in preclinical Alzheimer's disease detected using free water elimination diffusion tensor imaging. PLoS One 12:e0173982.

Huynh KM, Chen G, Wu Y, Shen D, Yap PT (2019) Multi-site harmonization of diffusion MRI data via method of moments. IEEE Trans Med Imaging 38:1599-1609.

Ito K, Ohtsuka C, Yoshioka K, Kameda H, Yokosawa S, Sato R, Terayama Y, Sasaki M (2017) Differential diagnosis of parkinsonism by a combined use of diffusion kurtosis imaging and quantitative susceptibility mapping. Neuroradiology 59:759-769.

Jelescu IO, Budde MD (2017) Design and validation of diffusion MRI models of white matter. Front Phys doi: 10.3389/fphy.2017.00061.

Jensen JH, Helpern JA (2010) MRI quantification of non-Gaussian water diffusion by kurtosis analysis. NMR Biomed 23:698-710.

Jensen JH, Helpern JA, Ramani A, Lu H, Kaczynski K (2005a) Diffusional kurtosis imaging: the quantification of non-gaussian water diffusion by means of magnetic resonance imaging. Magn Reson Med 53:1432-1440.

Ji F, Pasternak O, Liu S, Loke YM, Choo BL, Hilal S, Xu X, Ikram MK, Venketasubramanian N, Chen CL, Zhou J (2017) Distinct white matter microstructural abnormalities and extracellular water increases relate to cognitive impairment in Alzheimer's disease with and without cerebrovascular disease. Alzheimers Res Ther 9:63.

Ji F, Pasternak O, Ng KK, Chong JSX, Liu S, Zhang L, Shim HY, Loke YM, Tan BY, Venketasubramanian N, Chen CL, Zhou JH (2019) White matter microstructural abnormalities and default network degeneration are associated with early memory deficit in Alzheimer's disease continuum. Sci Rep 9:4749.

Kamagata K, Hatano T, Aoki S (2016a) What is NODDI and what is its role in Parkinson's assessment? Expert Rev Neurother 16:241-243.

Kamagata K, Hatano T, Okuzumi A, Motoi Y, Abe O, Shimoji K, Kamiya K, Suzuki M, Hori M, Kumamaru KK, Hattori N, Aoki S (2016b) Neurite orientation dispersion and density imaging in the substantia nigra in idiopathic Parkinson disease. Eur Radiol 26:2567-2577.

Kamagata K, Shimoji K, Hori M, Nishikori A, Tsuruta K, Yoshida M, Kamiya K, Irie R, Suzuki M, Kyogoku S, Suzuki Y, Sato N, Aoki S (2015) Intersite reliability of diffusion tensor imaging on two 3T scanners. Magn Reson Med Sci 14:227-233.

Kamagata K, Tomiyama H, Hatano T, Motoi Y, Abe O, Shimoji K, Kamiya K, Suzuki M, Hori M, Yoshida M, Hattori N, Aoki S (2014) A preliminary diffusional kurtosis imaging study of Parkinson disease: comparison with conventional diffusion tensor imaging. Neuroradiology 56:251-258.

Kamagata K, Tomiyama H, Motoi Y, Kano M, Abe O, Ito K, Shimoji K, Suzuki M, Hori M, Nakanishi A, Kuwatsuru R, Sasai K, Aoki S, Hattori N (2013) Diffusional kurtosis imaging of cingulate fibers in Parkinson disease: comparison with conventional diffusion tensor imaging. Magn Reson Imaging 31:1501-1506.

Kamagata K, Zalesky A, Hatano T, Di Biase MA, El Samad O, Saiki S, Shimoji K, Kumamaru KK, Kamiya K, Hori M, Hattori N, Aoki S, Pantelis C (2018) Connectome analysis with diffusion MRI in idiopathic Parkinson's disease: Evaluation using multi-shell, multi-tissue, constrained spherical deconvolution. Neuroimage Clin 17:518-529.

Kamagata K, Zalesky A, Hatano T, Ueda R, Di Biase MA, Okuzumi A, Shimoji K, Hori M, Caeyenberghs K, Pantelis C, Hattori N, Aoki S (2017) Gray matter abnormalities in idiopathic Parkinson's disease: evaluation by diffusional kurtosis imaging and neurite orientation dispersion and density imaging. Hum Brain Mapp 38:3704-3722.

Kim WH, Racine AM, Adluru N, Hwang SJ, Blennow K, Zetterberg H, Carlsson CM, Asthana S, Koscik RL, Johnson SC, Bendlin BB, Singh V (2019) Cerebrospinal fluid biomarkers of neurofibrillary tangles and synaptic dysfunction are associated with longitudinal decline in white matter connectivity: A multi-resolution graph analysis. Neuroimage Clin 21:101586.

Klingelhoefer L, Reichmann H (2017) Parkinson's disease as a multisystem disorder. J Neural Transm (Vienna) 124:709-713.

Mallio CA, Schmidt R, de Reus MA, Vernieri F, Quintiliani L, Curcio G, Beomonte Zobel B, Quattrocchi CC, van den Heuvel MP (2015) Epicentral disruption of structural connectivity in Alzheimer's disease. CNS Neurosci Ther 21:837-845.

Metzler-Baddeley C, O'Sullivan MJ, Bells S, Pasternak O, Jones DK (2012) How and how not to correct for CSF-contamination in diffusion MRI. NeuroImage 59:1394-1403.

Mitchell T, Archer DB, Chu WT, Coombes SA, Lai S, Wilkes BJ, McFarland NR, Okun MS, Black ML, Herschel E, Simuni T, Comella C, Xie T, Li H, Parrish TB, Kurani AS, Corcos DM, Vaillancourt DE (2019) Neurite orientation dispersion and density imaging (NODDI) and free-water imaging in Parkinsonism. Hum Brain Mapp 40:5094-5107.

Montal V, Vilaplana E, Alcolea D, Pegueroles J, Pasternak O, González-Ortiz S, Clarimón J, Carmona-Iragui M, Illán-Gala I, Morenas-Rodríguez E, Ribosa-Nogué R, Sala I, Sánchez-Saudinós MB, García-Sebastian M, Villanúa J, Izagirre A, Estanga A, Ecay-Torres M, Iriondo A, Clerigue M, et al. (2018) Cortical microstructural changes along the Alzheimer's disease continuum. Alzheimers Dement 14:340-351.

Mori S, Zhang J (2006) Principles of diffusion tensor imaging and its applications to basic neuroscience research. Neuron 51:527-539.

Nigro S, Riccelli R, Passamonti L, Arabia G, Morelli M, Nistico R, Novellino F, Salsone M, Barbagallo G, Quattrone A (2016) Characterizing structural neural networks in de novo Parkinson disease patients using diffusion tensor imaging. Hum Brain Mapp 37:4500-4510.

Oestreich LKL, Lyall AE, Pasternak O, Kikinis Z, Newell DT, Savadjiev P, Bouix S, Shenton ME, Kubicki M, Australian Schizophrenia Research B, Whitford TJ, McCarthy-Jones S (2017) Characterizing white matter changes in chronic schizophrenia: A free-water imaging multi-site study. Schizophr Res 189:153-161.

Ofori E, Krismer F, Burciu RG, Pasternak O, McCracken JL, Lewis MM, Du G, McFarland NR, Okun MS, Poewe W, Mueller C, Gizewski ER, Schocke M, Kremser C, Li H, Huang X, Seppi K, Vaillancourt DE (2017) Free water improves detection of changes in the substantia nigra in parkinsonism: A multisite study. Mov Disord 32:1457-1464.

Ofori E, Pasternak O, Planetta PJ, Burciu R, Snyder A, Febo M, Golde TE, Okun MS, Vaillancourt DE (2015a) Increased free water in the substantia nigra of Parkinson's disease: a single-site and multi-site study. Neurobiol Aging 36:1097-1104.

Ofori E, Pasternak O, Planetta PJ, Li H, Burciu RG, Snyder AF, Lai S, Okun MS, Vaillancourt DE (2015b) Longitudinal changes in free-water within the substantia nigra of Parkinson's disease. Brain 138:2322-2331.

Parente DB, Gasparetto EL, da Cruz LC, Jr., Domingues RC, Baptista AC, Carvalho AC, Domingues RC (2008) Potential role of diffusion tensor MRI in the differential diagnosis of mild cognitive impairment and Alzheimer's disease. AJR Am J Roentgenol 190:1369-1374.

Parker TD, Slattery CF, Zhang J, Nicholas JM, Paterson RW, Foulkes AJM, Malone IB, Thomas DL, Modat M, Cash DM, Crutch SJ, Alexander DC, Ourselin S, Fox NC, Zhang H, Schott JM (2018) Cortical microstructure in young onset Alzheimer's disease using neurite orientation dispersion and density imaging. Hum Brain Mapp 39:3005-3017.

Parvathaneni P, Nath V, Blaber JA, Schilling KG, Hainline AE, Mojahed E, Anderson AW, Landman BA (2018) Empirical reproducibility, sensitivity, and optimization of acquisition protocol, for Neurite Orientation Dispersion and Density Imaging using AMICO. Magn Reson Imaging 50:96-109.

Pasternak O, Sochen N, Gur Y, Intrator N, Assaf Y (2009) Free water elimination and mapping from diffusion MRI. Magn Reson Med 62:717-730.

Petersen RC (2004) Mild cognitive impairment as a diagnostic entity. J Intern Med 256:183-194.

Petersen RC (2009) Early diagnosis of Alzheimer's disease: is MCI too late? Curr Alzheimer Res 6:324-330.

Petersen RC, Aisen PS, Beckett LA, Donohue MC, Gamst AC, Harvey DJ, Jack CR, Jr., Jagust WJ, Shaw LM, Toga AW, Trojanowski JQ, Weiner MW (2010) Alzheimer's Disease Neuroimaging Initiative (ADNI): clinical characterization. Neurology 74:201-209.

Planetta PJ, Ofori E, Pasternak O, Burciu RG, Shukla P, DeSimone JC, Okun MS, McFarland NR, Vaillancourt DE (2016) Free-water imaging in Parkinson's disease and atypical parkinsonism. Brain 139:495-508.

Reid BE, Di Biase MA, Pomper MG, Shenton ME, Du Y, Coughlin JM, Pasternak O (2019) Examining links between free water and a TSPO-PET marker of neuroinflammation. In: ISMRM 27th Annual Meeting and Exhibition. Montreal, Canada.

Salloway S, Sperling R, Fox NC, Blennow K, Klunk W, Raskind M, Sabbagh M, Honig LS, Porsteinsson AP, Ferris S, Reichert M, Ketter N, Nejadnik B, Guenzler V, Miloslavsky M, Wang D, Lu Y, Lull J, Tudor IC, Liu E, et al. (2014) Two phase 3 trials of bapineuzumab in mild-to-moderate Alzheimer's disease. N Engl J Med 370:322-333.

Salsone M, Labate A, Quattrone A (2012) Cardiac denervation precedes nigrostriatal damage in idiopathic rapid eye movement sleep behavior disorder. Mov Disord 27:1068-1069.

Schapira AHV, Chaudhuri KR, Jenner P (2017) Non-motor features of Parkinson disease. Nat Rev Neurosci 18:435-450.

Schmand B, Huizenga HM, van Gool WA (2010) Meta-analysis of CSF and MRI biomarkers for detecting preclinical Alzheimer's disease. Psychol Med 40:135-145.

Shahim P, Holleran L, Kim JH, Brody DL (2017) Test-retest reliability of high spatial resolution diffusion tensor and diffusion kurtosis imaging. Sci Rep 7:11141.

Slattery CF, Zhang J, Paterson RW, Foulkes AJM, Carton A, Macpherson K, Mancini L, Thomas DL, Modat M, Toussaint N, Cash DM, Thornton JS, Henley SMD, Crutch SJ, Alexander DC, Ourselin S, Fox NC, Zhang H, Schott JM (2017) ApoE influences regional white-matter axonal density loss in Alzheimer's disease. Neurobiol Aging 57:8-17.

Soares JM, Marques P, Alves V, Sousa N (2013) A hitchhiker's guide to diffusion tensor imaging. Front Neurosci 7:31.

Song GP, Yao TT, Wang D, Li YH (2019) Differentiating between Alzheimer's disease, amnestic mild cognitive impairment, and normal aging via diffusion kurtosis imaging. Neural Regen Res 14:2141-2146.

Soto C, Pritzkow S (2018) Protein misfolding, aggregation, and conformational strains in neurodegenerative diseases. Nat Neurosci 21:1332-1340.

Steven AJ, Zhuo J, Melhem ER (2014) Diffusion kurtosis imaging: an emerging technique for evaluating the microstructural environment of the brain. AJR Am J Roentgenol 202:26-33.

Struyfs H, Van Hecke W, Veraart J, Sijbers J, Slaets S, De Belder M, Wuyts L, Peters B, Sleegers K, Robberecht C, Van Broeckhoven C, De Belder F, Parizel PM, Engelborghs S (2015) Diffusion kurtosis imaging: a possible MRI biomarker for AD diagnosis? J Alzheimers Dis 48:937-948.

Surova Y, Lampinen B, Nilsson M, Latt J, Hall S, Widner H, Swedish Bio Fs, van Westen D, Hansson O (2016) Alterations of diffusion kurtosis and neurite density measures in deep grey matter and white matter in Parkinson's disease. PLoS One 11:e0157755.

Szczepankiewicz F, Latt J, Wirestam R, Leemans A, Sundgren P, van Westen D, Stahlberg F, Nilsson M (2013) Variability in diffusion kurtosis imaging: impact on study design, statistical power and interpretation. Neuroimage 76:145-154.

Wang D, Guo ZH, Liu XH, Li YH, Wang H (2015a) Examination of hippocampal differences between Alzheimer disease, amnestic mild cognitive impairment and normal aging: diffusion kurtosis. Curr Alzheimer Res 12:80-87.

Wang ML, Wei XE, Fu JL, Li W, Yu MM, Li PY, Li WB (2018) Subcortical nuclei in Alzheimer's disease: a volumetric and diffusion kurtosis imaging study. Acta Radiol 59:1365-1371.

Wang WY, Yu JT, Liu Y, Yin RH, Wang HF, Wang J, Tan L, Radua J, Tan L (2015b) Voxel-based meta-analysis of grey matter changes in Alzheimer's disease. Transl Neurodegener 4:6.

Wang Y, Wang Q, Haldar JP, Yeh FC, Xie M, Sun P, Tu TW, Trinkaus K, Klein RS, Cross AH, Song SK (2011) Quantification of increased cellularity during inflammatory demyelination. Brain 134:3590-3601.

Wheeler-Kingshott CA, Cercignani M (2009) About "axial" and "radial" diffusivities. Magn Reson Med 61:1255-1260.

Yang J, Archer DB, Burciu RG, Muller M, Roy A, Ofori E, Bohnen NI, Albin RL, Vaillancourt DE (2019) Multimodal dopaminergic and free-water imaging in Parkinson's disease. Parkinsonism Relat Disord 62:10-15.

Yu P, Sun J, Wolz R, Stephenson D, Brewer J, Fox NC, Cole PE, Jack CR Jr, Hill DL, Schwarz AJ; Coalition Against Major Diseases and the Alzheimer's Disease Neuroimaging Initiative (2014) Operationalizing hippocampal volume as an enrichment biomarker for amnestic mild cognitive impairment trials: effect of algorithm, test-retest variability, and cut point on trial cost, duration, and sample size. Neurobiol Aging 35:808-818.

Yuan L, Sun M, Chen Y, Long M, Zhao X, Yin J, Yan X, Ji D, Ni H (2016) Non-Gaussian diffusion alterations on diffusion kurtosis imaging in patients with early Alzheimer's disease. Neurosci Lett 616:11-18.

Zhang G, Zhang C, Wang Y, Wang L, Zhang Y, Xie H, Lu J, Nie K (2019) Is hyperhomocysteinemia associated with the structural changes of the substantia nigra in Parkinson's disease? A two-year follow-up study. Parkinsonism Relat Disord 60:46-50.

Zhang G, Zhang Y, Zhang C, Wang Y, Ma G, Nie K, Xie H, Liu J, Wang L (2015) Diffusion kurtosis imaging of substantia nigra is a sensitive method for early diagnosis and disease evaluation in Parkinson's disease. Parkinsons Dis 2015:207624.

Zhang G, Zhang Y, Zhang C, Wang Y, Ma G, Nie K, Xie H, Liu J, Wang L (2016) Striatal silent lacunar infarction is associated with changes to the substantia nigra in patients with early-stage Parkinson's disease: A diffusion kurtosis imaging study. J Clin Neurosci 33:138-141.

Zhang H, Schneider T, Wheeler-Kingshott CA, Alexander DC (2012) NODDI: practical in vivo neurite orientation dispersion and density imaging of the human brain. Neuroimage 61:1000-1016.

Zhu T, Hu R, Qiu X, Taylor M, Tso Y, Yiannoutsos C, Navia B, Mori S, Ekholm S, Schifitto G, Zhong J (2011) Quantification of accuracy and precision of multi-center DTI measurements: a diffusion phantom and human brain study. Neuroimage 56:1398-1411.

Zhuo J, Xu S, Proctor JL, Mullins RJ, Simon JZ, Fiskum G, Gullapalli RP (2012) Diffusion kurtosis as an in vivo imaging marker for reactive astrogliosis in traumatic brain injury. Neuroimage 59:467-477.